

## Direct phase measurement of aspheric surface contours

Katherine Creath and James C. Wyant

WYKO Corporation, 2990 E. Ft. Lowell Road, Tucson, Arizona 85716

### Abstract

Two-wavelength holography and phase-shifting interferometry are combined to measure aspheric surface contours with a variable sensitivity. In this technique, the surface is effectively tested at a synthesized longer equivalent wavelength  $\lambda_{eq} = \lambda_a \lambda_b / |\lambda_a - \lambda_b|$  using measurements made at wavelengths  $\lambda_a$  and  $\lambda_b$  where the difference of the phases measured for  $\lambda_a$  and  $\lambda_b$  yields the modulo  $2\pi$  phase at  $\lambda_{eq}$ . A mask of point apertures is placed over the detector array in order to resolve closely spaced fringes. This technique has an rms repeatability of  $\lambda_{eq}/100$ . Limits to this technique are discussed and results are shown.

### Introduction

Aspheric optical components are rapidly becoming important to the optical designer. Often the performance of an optical system will depend on whether it is possible to generate and test an aspheric component. Until recently, means of generating steep aspherics have not been available. However, with the advent of new techniques such as diamond-point machining,<sup>1</sup> bend and polish,<sup>2</sup> and computer-controlled curve generators,<sup>3-4</sup> aspherics are now more feasible. The missing link in aspheric production is the measurement of a surface to know what shape has been generated.

Currently, aspherics are tested using a number of different techniques such as null lenses and computer-generated holograms.<sup>5</sup> A null lens is designed to compensate for the departure of the test surface from a spherical surface. Each asphere requires a different null lens containing a large number of elements which must be tested individually as well as a system. A computer-generated hologram serves the same purpose, but the wavefront is produced by a hologram which has been computer-calculated and drawn using some sort of plotting device. This technique also produces a one-of-a-kind test, and it is not always possible to obtain a suitable low-distortion hologram from a plotter. Both of these techniques involve a lot of design for each asphere tested, can be quite expensive, and are time-consuming. Other techniques for testing aspheres include mechanical means (such as a stylus), and shearing interferometry. Mechanical means cannot yield a high enough precision, and shearing generally only gives information in one direction so that an integration is needed to determine surface shape.

Another technique worth mentioning is two-wavelength holography (TWH) which uses two visible wavelengths to produce a long effective wavelength for wavefront contouring of any surface, rough or smooth.<sup>6</sup> It is a good technique for testing aspheres and steep surfaces because of its variable sensitivity; however, it is not very precise, and requires an intermediate holographic recording. TWH has also been combined with phase-shifting interferometry producing a high precision test.<sup>7</sup> In this technique, a hologram made at one wavelength is illuminated with a second wavelength. The relative phase in the interferometer is then shifted at the second wavelength and the phase at a longer, less sensitive, equivalent wavelength can be determined. This technique is a good step beyond TWH, but it requires making an intermediate hologram before interferogram data is recorded to calculate phase.

A simple means of testing a surface with a large departure from a spherical surface is in great need. Such a system needs to be as flexible in testing aspheres as a Twyman-Green interferometer is in testing spheres. It should also not need intermediate recordings or the generation of holograms to produce an interferogram of the test surface. Two-wavelength phase-shifting interferometry (TWPSI) is such a technique.<sup>8-9</sup> Surface height variations of optically smooth surfaces can be determined from the phase data by utilizing computers to record data and calculate surface errors. This technique is fast and has no intermediate recording step. With TWPSI, it is possible to directly measure the profiles of deeper surfaces than is possible with a single wavelength by applying phase measurement to two-wavelength holography.

### Theory

In TWH the interferogram at one wavelength  $\lambda_a$  is recorded on photographic film with the test surface in place, developed, placed back in the original position, and then illuminated with the interferogram produced by a different wavelength  $\lambda_b$  of the same surface. The interference pattern between these two interferograms is then spatially filtered to remove unwanted components. The result of this test is an interferogram in which fringes are spaced as if the surface were tested with an equivalent wavelength given by <sup>6</sup>

$$\lambda_{eq} = \frac{\lambda_a \lambda_b}{|\lambda_a - \lambda_b|} \quad (1)$$

The sensitivity of the test can be varied by changing the two illuminating wavelengths. When the wavelengths used are produced by argon-ion and HeNe lasers, the equivalent wavelength can be varied over a range of 2 to 50  $\mu\text{m}$ .

Phase-shifting interferometry (PSI) is a technique which can determine the shape of a surface or wavefront by calculating a phase map from the measured intensities. The phase information is obtained by shifting the phase of one beam in the interferometer by a known amount and measuring the intensity in the interferogram for many different phase shifts. For the phase calculations used in this paper, the intensity is integrated over the time it takes to move a reference mirror linearly through a  $2\alpha$  change in phase (usually near  $90^\circ$ ) with a piezo-electric transducer (PZT). Four frames of intensity data are recorded in this manner:<sup>10</sup>

$$\begin{aligned} A(x,y) &= I_0[1 + \gamma\cos(\phi(x,y) - 3\alpha)] \\ B(x,y) &= I_0[1 + \gamma\cos(\phi(x,y) - \alpha)] \\ C(x,y) &= I_0[1 + \gamma\cos(\phi(x,y) + \alpha)] \\ D(x,y) &= I_0[1 + \gamma\cos(\phi(x,y) + 3\alpha)] \end{aligned} \quad (2)$$

where  $I_0$  is the average intensity, and  $\gamma$  is the modulation of the interference term. The phase  $\phi$  is calculated using

$$\phi = \arctan \left[ \frac{\sqrt{[(A-D) + (B-C)][3(B-C) - (A-D)]}}{(B+C) - (A+D)} \right] \quad (3)$$

at each detected point in the interferogram. The calculation of the phase is independent of the actual amount the phase is shifted as long as it is linear and  $\alpha$  is constant. This enables the same equations to be used at many different wavelengths without changing the ramping voltage to the PZT.

The optical path difference (OPD) between the reference and object wavefronts is given by

$$OPD(x,y) = \frac{\phi(x,y) \lambda}{2\pi} \quad (4)$$

where  $\lambda$  is the effective wavelength for the phase  $\phi$ . OPD is related to object surface height by a multiplicative factor, which is one-half for a double-pass interferometer like the Twyman-Green.  $2\pi$  phase ambiguities are smoothed by comparing adjacent pixels and adding or subtracting multiples of  $2\pi$  until the difference between adjacent pixels is less than  $\pi$ . The wavefront's phase between adjacent pixels must not change by more than  $\pi$  (one-half wave of OPD) for the  $2\pi$  ambiguities to be handled correctly. This limits the number of fringes measurable across the test surface, thereby governing the test sensitivity.

Extension of the measurement range of phase-shifting interferometry over the range of two-wavelength holography requires a closer look at TWH. The interferogram obtained with two-wavelengths in TWH has an intensity distribution given by<sup>6</sup>

$$I(x,y) = 1 + \cos \left[ 2\pi \text{OPD}(x,y) \left[ \frac{1}{\lambda_a} - \frac{1}{\lambda_b} \right] \right] \quad (5)$$

where this expression assumes unit amplitudes, no tilt between the object and reference beams, and OPD refers to the optical path difference. The phase is given by the argument of the cosine term and can be written as

$$\phi_{eq}(x,y) = \frac{2\pi \text{OPD}(x,y)}{\lambda_{eq}} = \phi_a(x,y) - \phi_b(x,y) \quad (6)$$

where  $\phi_a$  and  $\phi_b$  are the phases measured for  $\lambda_a$  and  $\lambda_b$ . The difference of the phases measured at the two wavelengths yields the phase associated with the equivalent wavelength. In order to remove  $2\pi$  ambiguities from the equivalent wavelength data, the phase difference between two adjacent pixels of the equivalent phase must be less than  $\pi$  ( $\lambda_{eq}/2$  in OPD).

To measure phase at an effective wavelength  $\lambda_{eq}$  using two shorter wavelengths under computer control, the following algorithm is used. First, the computer takes four frames of data at  $\lambda_a$  while shifting the phase in the interferometer. Next, the phase shifter is returned to its original position, the illumination is switched from  $\lambda_a$  to  $\lambda_b$ , and four more data frames are taken while shifting the phase the same as for  $\lambda_a$ . The phases  $\phi_a$  and  $\phi_b$  are calculated modulo  $2\pi$  using Eq. (3) and then subtracted to yield  $\phi_{eq}$  modulo  $2\pi$ . Phase ambiguities are then removed using an integration routine. This approach is very simple, and easily implemented using existing phase-measurement equipment.

#### Limitations to TWPSI

There are three limitations which need to be considered. Firstly, steep surfaces cause very closely spaced fringes which may not be resolvable by the detector. Therefore, a modulation of the fringe intensity may not be detected resulting in phase calculation errors. Secondly, the uncertainty in the measurement is proportional to the equivalent wavelength. This causes the signal-to-noise ratio of the measurement to be reduced at longer wavelengths. Finally, chromatic aberrations in the system cause errors and lots of "noise" in the equivalent wavelength measurement. Ways of reducing these limitations are discussed in this section.

When a fringe pattern is recorded by a detector array, discrete voltages are output representing the average intensity incident upon the detector element over the integration time. As the relative phase between the object and reference beams is shifted, the intensities read by point detectors should change as shown in Fig. 1a. If the interference data are sampled such that there are two detector elements for each fringe (each half-wave of OPD), then the wavefront can be reconstructed. However, if the fringe pattern is not sufficiently sampled, the wavefront cannot be correctly reconstructed as shown in Fig. 1b where there is more than 1/2 fringe per detector. When the area of the detector is finite, the detector reads the average fringe intensity over its area as shown in Fig. 1c. As long as there is less than one-half of a fringe per detector element, the intensity will be modulated. However, if there is 1 fringe over the area of the detector element there will be no modulation (Fig. 1d). Thus, the detector size influences the recorded fringe modulation, whereas the detector spacing determines if the wavefront can be reconstructed without phase ambiguities.

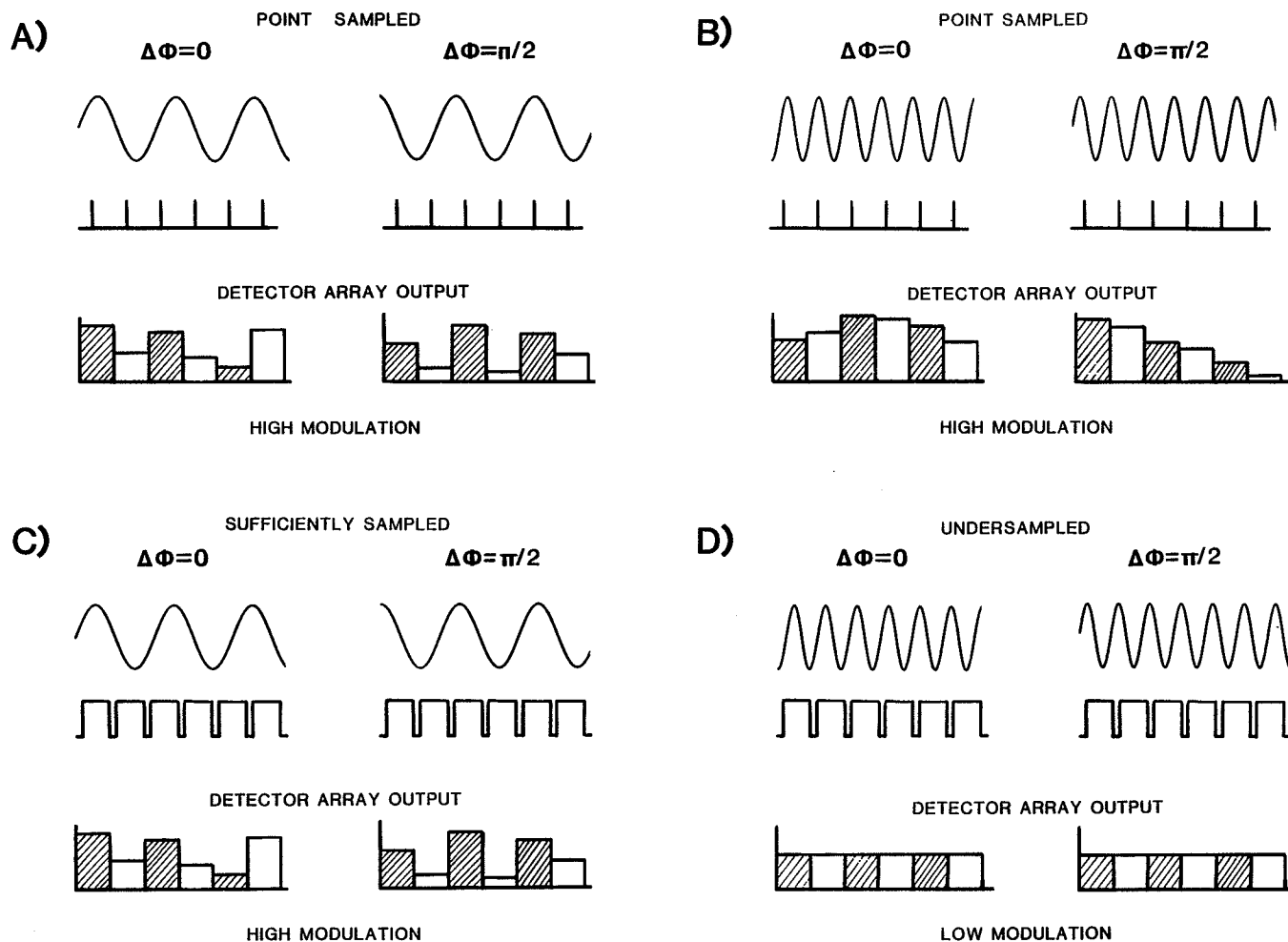


**Figure 1:** A) Sufficient sampling with point detectors showing high modulation of the intensity as the interferometer's relative phase is shifted by  $\pi/2$ . B) Undersampling with point detectors showing aliasing of fringe pattern with detector spacing where wavefront cannot be reconstructed. C) Sufficient sampling with finite-sized detectors with  $<1/2$  fringe over the detector area. D) Undersampling with finite-sized detectors showing no intensity modulation.

Fringe modulation is a fundamental problem in all phase-shifting techniques<sup>8,11</sup> making the ratio of the detector size to the fringe spacing important. If many fringes are incident upon a single detector element, the intensity measured will be an average over the detector area. When the phase is shifted, these points will not be modulated sufficiently to get an accurate phase reading. The modulation  $\gamma$  of a detected point is determined using

$$\gamma = \sqrt{I_1 I_2} = \frac{1}{2} \sqrt{\frac{[(B-C) + (A-D)]^2 + [(B+C) - (A+D)]^2}{2}}, \quad (7)$$

where  $2\alpha$  is assumed to be near  $90^\circ$ . If the modulation of a data point is less than a threshold  $I_{\min}$ , that data point is flagged as bad; otherwise, the point is considered good and the phase of the wavefront is calculated at that point. In the examples shown in the next section, there are detector points where this occurs. These

points are discarded during the calculations using Eq. (7). The spacing between detectors dictates the ultimate measurement sensitivity because of the  $2\pi$  ambiguities; but this can be overcome by simply changing the equivalent wavelength.

To ensure sufficient sampling to yield high intensity modulation as the phase is shifted, the size of the detector should be small compared to the fringe spacing. This is accomplished by imaging a mask of small apertures onto the face of the detector array. The mask in Fig. 2 consists of  $5\ \mu\text{m}$  square apertures separated by the detector spacing.

The signal-to-noise (S/N) ratio of the equivalent wavelength phase data depends upon the wavelength. If there are 10 waves of departure at a wavelength of 500 nm, there will be only 1/2 of a wave departure at an equivalent wavelength of 10  $\mu\text{m}$ . Phase-shifting techniques are usually precise (or repeatable) to an rms of about  $\lambda/100$ , and the precision is proportional to the effective wavelength of the measurement. At 500 nm  $\lambda/100$  will be 5 nm meaning that features smaller than 5 nm in extent cannot be measured. At 10  $\mu\text{m}$   $\lambda/100$  precision would be 100 nm. Thus, a S/N ratio of 1000 at 5 nm ends up as a S/N of 5 at 10  $\mu\text{m}$ . This scaling has been referred to as an error magnification,<sup>8</sup> and is proportional to the square of the ratio of the two wavelengths. If ambiguities in the single wavelength measurement can be resolved by comparison to the equivalent wavelength data, the signal-to-noise ratio of the measurement can be significantly enhanced.

The largest errors in the phase maps can be attributed to chromatic aberration. Any glass elements in the interferometer will have dispersion which may produce a wavelength dependence of the system aberrations. When the interferograms change size or shift laterally with wavelength because of chromatic aberration, the equivalent wavelength phase can have errors due to lack of a point-by-point correspondence between the phase maps at each wavelength. To reduce errors due to chromatic aberration, all glass elements should be achromatized for the wavelengths in use. A small amount of chromatic aberration can be tolerated, but it should not shift the location of the incident fringes by more than one-half of a fringe or change the size of the interferogram by more than a pixel in order to have good results.

If the interferometer is corrected for the two colors in use, the equivalent wavelength data can be directly used to remove ambiguities in one of the single-wavelength phase measurements. As long as the noise due to chromatic aberration is less than one-half of the measurement wavelength ( $\lambda_a$  or  $\lambda_b$ ), then the number of  $2\pi$ 's to add to the single-wavelength measurement can be determined by direct point-by-point comparison with the integrated equivalent wavelength phase. If a direct comparison is not possible, the equivalent wavelength data can be modified by removing the tilt and piston due to chromatic before correction.<sup>12</sup>

Thus, the limitations to TWPSI can be reduced by using a mask of point apertures to increase intensity modulation, correcting the interferometer for chromatic aberration, and by correcting ambiguities in the single-wavelength data using the equivalent wavelength data as a reference. This enables the wavefront phase to be reconstructed over the range of the equivalent wavelength test, and have the precision obtainable using a shorter measurement wavelength.

### Experiment

To illustrate this technique, phases of steep wavefronts were measured using a Twyman-Green interferometer (Fig. 3) with a PMS tunable HeNe laser source. A test surface is placed in one arm of the interferometer, and a flat mirror controlled by a PZT is placed in the other. An achromatic diverging lens is used to match the curvature of the base sphere for the aspheric surface. Interferograms are recorded using a Reticon 100x100 diode array with a fiber optic window coupled to an HP-320 computer. The fiber optic window is used to enable the mask to be imaged directly onto the detector array when it is placed in contact with the window. A zoom lens images the test surface onto the fiber window. The wavelengths used in this experiment are 594 nm, 604 nm, 612 nm, and 633 nm from the tunable HeNe laser yielding the equivalent wavelengths shown in Table 1.

Table 1: Equivalent wavelengths using PMS tunable HeNe laser.

$\lambda_{eq}(\mu\text{m})$	0.633	0.612	0.604	0.594
0.633	---	18.527	13.271	9.714
0.612	18.527	---	46.783	20.423
0.604	13.271	46.783	---	36.246
0.594	9.714	20.423	36.246	---

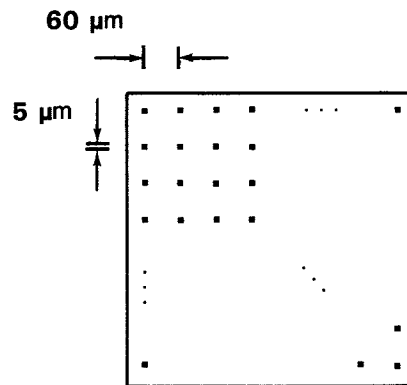


Figure 2: Mask of  $5\ \mu\text{m}$  square apertures separated by detector spacing used to increase the modulation of closely spaced fringes.

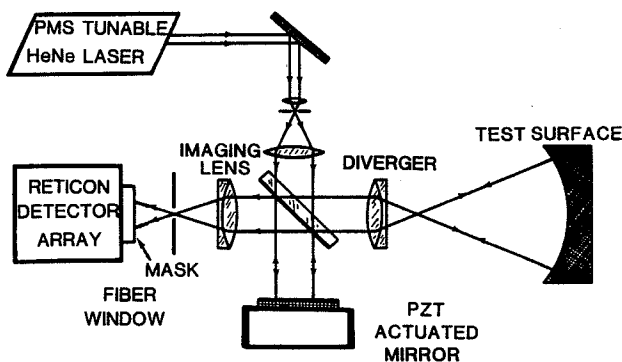


Figure 3: Experimental setup for testing an aspheric surface using two-wavelength phase-shifting interferometry.

Fig. 4 shows the interferogram of the aspheric surface under test at 633 nm. When this surface is tested using data at a single wavelength, there are ambiguities in the phase which cannot be resolved (see Fig. 5). This is because the OPD of the wavefront is changing by more than one-half of the measurement wavelength between adjacent detector elements. When modulo  $2\pi$  phase measurements are taken at wavelengths of 633 nm and 594 nm and then subtracted, phase ambiguities can be resolved as shown in Fig. 6a. At the equivalent wavelength of 9.7  $\mu\text{m}$ , the asphere has a peak-to-valley (P-V) departure of 0.867 waves and an rms of 0.119. Since phase ambiguities are resolvable, the OPD must be changing by less than half a wave between adjacent detector elements.

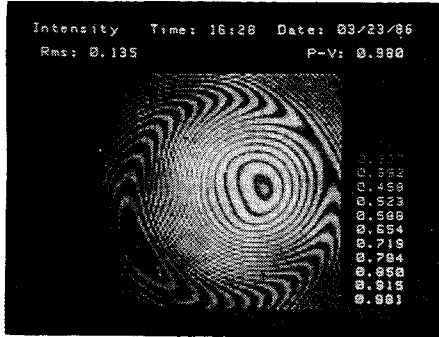


Figure 4: Interferogram of aspheric surface under test at 633 nm.

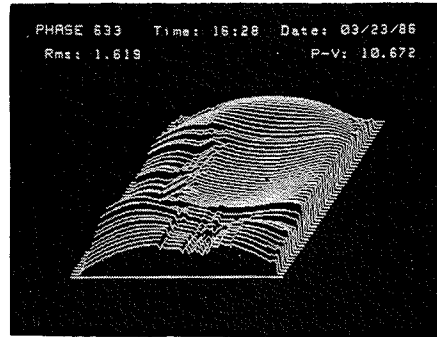


Figure 5: Result of trying to remove ambiguities in the phase calculated at 633 nm from surface of Fig. 4.

With the PMS laser many different equivalent wavelengths can be obtained. Figure 6 shows the same test surface as measured at three different equivalent wavelengths. Note that as the equivalent wavelength is increased, the noise also increases. This is due to the error magnification. The noise in the interferometer system is measured to be about  $\lambda/15$  in (P-V), and  $\lambda/100$  in rms independent of what wavelength is used. Thus, as the equivalent wavelength gets longer, the P-V of the test surface will get smaller as will the signal-to-noise ratio. At  $\lambda_{eq}=20.4 \mu\text{m}$ , the P-V of 0.332 waves and rms of 0.052 waves scale well in comparison to the results at 9.7  $\mu\text{m}$ . If a real steep surface were measured, one could take measurements at a series of wavelengths and work backwards through shorter and shorter equivalent wavelengths until ambiguities in the single wavelength phase were corrected.<sup>13</sup>

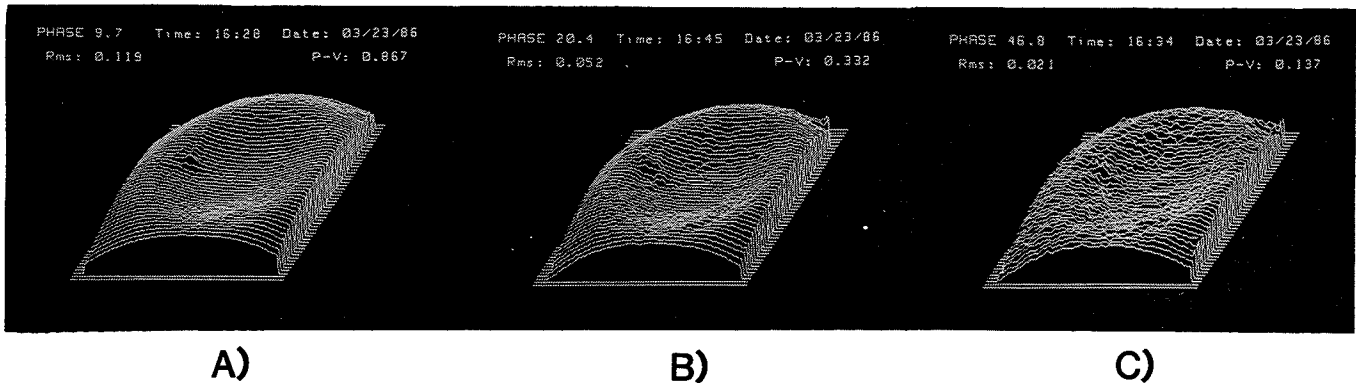


Figure 6: Calculated phase at different equivalent wavelengths for surface of Fig. 4 showing magnification of noise with wavelength. A)  $\lambda_{eq}=9.7 \mu\text{m}$ . B)  $\lambda_{eq}=20.4 \mu\text{m}$ . C)  $\lambda_{eq}=46.8 \mu\text{m}$ .

### Conclusions

Two-wavelength techniques are very valuable for the testing of steep surfaces such as aspheres because of the variable measurement sensitivity attainable by changing the wavelengths. The technique presented in this paper is very straightforward and easy to implement. Its precision is limited by the equivalent wavelength. In order to increase the precision of the measurement, the single-wavelength phase data can have its  $2\pi$  ambiguities resolved using the integrated two-wavelength phases. The range of the measurement can be increased by using point detectors to sample fringes with a closer spacing than the detector size. Since the interferograms at each wavelength are recorded and then combined inside the computer, the intermediate recording step of two-wavelength holography is unneeded. This makes the technique a more convenient means of testing than TWH. Using the computer means there are no errors due to fringe digitization, and further analysis on the phase data may easily be done. The technique of manipulating primary interferograms inside a computer to produce a secondary interferogram from double-exposure measurements has many applications besides TWPSI, one of which is phase measurement with double-exposure holography.

### Acknowledgements

The authors wish to thank Bob Huseman of EG&G Reticon and Ken Sample of PMS for their assistance.

### References

1. T. T. Saito, "Diamond turing of optics: past, present, exciting future," *Opt. Eng.* **17**, 570 (1978).
2. J. Lubliner, and J. E. Nelson, "Stressed mirror polishing. I: A technique for producing nonaxisymmetric mirrors," *Appl. Opt.* **19**, 2332 (1980).
3. J. R. P. Angel, and R. E. Parks, "Generation of off-axis aspherics," *Proc. SPIE* **332**, 316 (1982).
4. R. E. Parks, "Parameters for large optics generation," *Proc. SPIE* **571**, 35 (1985).
5. J. C. Wyant, and K. Creath, "Recent advances in interferometric optical testing," *Laser Focus*, p. 118 (Nov. 1985).
6. J. C. Wyant, "Testing Aspherics Using Two-Wavelength Holography," *Appl. Opt.* **10**, 2113 (1971).
7. J. C. Wyant, B. F. Oreb, and P. Hariharan, "Testing aspherics using two-wavelength holography: use of digital electronic techniques," *Appl. Opt.* **7**, 2107 (1968).
8. Y.-Y. Cheng, and J. C. Wyant, "Two-wavelength phase shifting interferometry," *Appl. Opt.* **23**, 4539 (1984).
9. K. Creath, Y.-Y. Cheng, and J. C. Wyant, "Contouring spheric surfaces using two-wavelength phase-shifting interferometry," *Opt. Acta* **32**, 1455 (1985).
10. P. Carré, "Installation et utilisation du comparateur photoelectrique et interferential du Bureau International des Poids et Mesures," *Metrologia* **2**, 13 (1966).
11. K. Creath, "Phase-shifting speckle interferometry," *Appl. Opt.* **24**, 3053 (1985).
12. K. Creath, "Testing aspheric surfaces using two-wavelength phase-shifting interferometry," *J. Opt. Soc. Am. A* **2**(13), P58 (1985).
13. Y.-Y. Cheng, and J. C. Wyant, "Multiple-wavelength phase-shifting interferometry," *Appl. Opt.* **24** 804 (1985).